ECTI Transactions on Computer and Information Technology
Journal homepage: https://ph01.tci-thaijo.org/index.php/ecticit/
Published by the ECTI Association, Thailand, ISSN: 2286-9131

Exploiting Impact of Imperfect CSI on Performance of Backscatter-Aided NOMA System

Minh-Sang Van Nguyen[1] and Dinh-Thuan Do[2,3]

ABSTRACT

In this paper, we consider the impact of imperfect channel state information (CSI) on outage probability of users in an ambient backscatter (AB) enabled nonorthogonal multiple access (NOMA) network. In our proposed scheme, a source node communicates with two destinations via a radio frequency-powered device. Such device is assume with ability of backscattering the signals from the base station. We derive expressions to show outage probability of main nodes in such system. The analytical expressions for the outage probability are checked with Monte-Carlo simulations. It has been shown that the analytical results match the simulation results. In particular, the user with higher allocated power exhibits its performance better than another 10%-15% when signal to noise ratio (SNR) at the source node is 30 dB.

Article information:

Keywords: Non-orthogonal Multiple Access (NOMA), Backscatter, Outage Probability

Article history:
Received: January 10, 2021
Revised: May 10, 2021
Accepted: May 20, 2021
Published: March 5, 2022 (Online)

DOI: 10.37936/ecti-cit.2022161.243828

1. INTRODUCTION

The deployment of the backscattering technology, namely backscatter communications (BC), has been thoroughly investigated in the literature [1–7]. In particular, by exploiting the incident radio-frequency (RF) signals, the backscatter device (*BD*) in BC modulates its own information before reflecting the modulated signals to the corresponding receiver. Therefore, the *BD* does not require the power-consuming active components such as analog-to-digital/digital-to-analog converters, oscillators. To implement low data rate networks, AB communication is proposed as promising transmission approach. As main advanatge, the AB devices do not need any supply infrastructure/specific power storage [1–4]. Once data transmission is required for the backscattering procedure, the AB transmitter (AB-Tx) switches its modes including the non-reflect and reflect modes (which correspond to the bits '0' and '1', respectively). To decode the information from the received backscattered signals, the envelope detection and averaging techniques are employed at the AB receiver (AB-Rx) [2]. The AB can be easily implemented together with any wireless communication node since AB can be deployed without complex circuitry and encoding/decoding schemes [3, 6]. As main characteristic, the operation of BC depends on the existence of RF signals and the active components. As a result, the BC is normarlly co-deployed with existing communication systems. The authors in [3] explored prototype example of a full duplex AB, in which a WiFi AP decodes the backscatter signals reflected by different IoT sensors while it transmits signals to normal WiFi clients in the same time. However, the availability of the ambient RF signals results in the performance of the backscatter communication since AB depends on the ambient nature of signals.

Regarding power consumption, a *BD* can Operate at low power as several μW [8]. The authors in [9] introduced where the secondary receiver is co-located with the primary receiver to form BC-aided cognitive radio. In such a network, the weighted sum-rate of both the secondary and primary links are maximized. In [10], to achieve optimal ergodic capacity in the spectrum sharing system, the reflection coefficient of *BD* and the transmit power of the primary trans-

[1]The author is with Faculty of Electronics Technology, Industrial University of Ho Chi Minh City (IUH), Ho Chi Minh City, Vietnam, E-mail: nguyenvanminhsang@iuh.edu.vn
[2]The author is with Future Networking Research Group, Ton Duc Thang University, Ho Chi Minh City, Vietnam, E-mail: dodinhthuan@tdtu.edu.vn
[3]The author is with Faculty of Electrical and Electronics Engineering, Ton Duc Thang University, Ho Chi Minh City, Vietnam, E-mail: dodinhthuan@tdtu.edu.vn
Corresponding author: nguyenvanminhsang@iuh.edu.vn

mission were jointly optimized, while the BD's interference to the primary receiver is treated to be less than a predefined threshold. In [11], the cooperative backscatter system with a dedicated source node is studied to split each transmission into two time slots, and such system adopted the harvest-then-transmit (HTT) protocol. Further, by optimizing the time durations of two time Slots and the reflection coefficient, the authors examined maximized achieved rate. In several studies, cooperative backscatter communication systems has also been studied in term of the performance analysis. For example, the authors in [12] derived formulas of the outage probabilities for both BC and the legacy transmission (LT) with a couple of transmission modes. The authors in [13] presented system to select the backscatter link to minimize the outage probability of the backscatter receiver based on the optimal reflection coefficient. Due to the extra co-channel interference caused by the backscattered signals, the degraded performance can be reported in the above works [9–13]. Moreover, the backscatter-assisted systems that considers how to select the appropriate working mode between the active radio or passive radio, i.e., using batteries or BC in [11, 14] in terms of the outage performance and symbol error rate, respectively. Different from [10–13], reference [15] studied a decode-and-forward (DF) enabled one-way cooperative ambient backscatter communication (CABC) system. In the system reported in [16], the source node relies on a DF enabled relay node to send its information to the destination node while the tag embedded in the relay node can convey its own information to the associated source by backscattering the difference signal produced by the two hops. It is worth noting that the scheme in [16] deployed the unidirectional communication for both the relaying transmission (RT) and BC.

On the other hand, to help AB transmit signals to much more users, NOMA is proposed since NOMA is recognized as an important technique for future wireless communication systems. In such NOMA, the transmitter transmits signals to multiple users in the same radio resource, due to its appearing benefits such as support for massive connections and enhanced spectrum efficiency [17–19]. Specifically, by superposing the messages in power domain, one can delpoy systems, namely power-domain NOMA systems, multiple users share the same time-frequency resource block [19]. In this system, the successive interference cancellation technique is adopted in the receiver to cancel inter-user interference within the same cell [20, 21]. The studies in [22, 23] presented uplink and downlink NOMA to exhibit optimal user pairing schemes. The authors in [24] explored a NOMA-enhanced wireless powered communication system to find optimal time and power resource allocation. The authors in [25] explored the system's sum rate for millimeter-wave communication with assistance of NOMA approach.

Recently, the authors in [26] studied backscatter receiver to implement a NOMA-enhanced monostatic backscatter communication system with co-located carrier transmitter. They derived formulas of the outage probability and average number of successfully decoded bits. In [27], a NOMA-enhanced bistatic backscatter communication network was considered in terms of the throughput performance and its optimal value. Motivated by recent work [26, 27], this paper studies system performance of two users which benefit from both AB and NOMA techniques.

2. SYSTEM MODEL

In this section, we will provide a backscatter-NOMA model, which incorporates the IoT system with a symbiotic radio (SR) model, which are the special cases of the backscatter-NOMA system.

Table 1: *MATHEMATICAL NOTATIONS USED IN THIS ARTICLE.*

Symbol	Description
$\Pr(.)$	Probability of an event
$CN(x, y)$	Complex Gaussian distribution with mean x and variance y
$\mathrm{E}[.]$	Expectation operator
$\mathrm{Ei}(.)$	The exponential integral function
$K_1(.)$	The modified Bessel function
s_1	The messages with unit power transmitted to D_1
s_2	The messages with unit power transmitted to D_2
$v(t)$	The t-th symbol to be transmitted by BD
P	The total transmit power of the BS
ε_i	The power allocation parameters of s_i with $\sum_i^2 \varepsilon_i = 1, 0 \leq \varepsilon_i \leq 1$
ϕ	A complex reflection coefficient
w_1	The complex Gaussian noise at D_1 with $w_1 \sim CN\left(0, \varsigma^2\right)$
w_2	The complex Gaussian noise at D_2 with $w_2 \sim CN\left(0, \varsigma^2\right)$
h_{S1}	The channel responses from the BS to D_1 with $h_{S1} \sim CN(0, \lambda_{S1})$
h_{S2}	The channel responses from the BS to D_2 with $h_{S2} \sim CN(0, \lambda_{S2})$
h_{SB}	The channel responses from the BS to BD with $h_{SB} \sim CN(0, \lambda_{SB})$
g_{B1}	The channel responses from the BD to D_1 with $g_{B1} \sim CN(0, \lambda_{B1})$
g_{B2}	The channel responses from the BD to D_2 with $g_{B2} \sim CN(0, \lambda_{B2})$
τ_{S1}	The error term, which is typically modeled as a complex Gaussian distributed random variable with $CN(0, \kappa_{S1})$ [28], [29]
τ_{S2}	The error term, which is typically modeled as a complex Gaussian distributed random variable with $CN(0, \kappa_{S2})$ [28], [29]

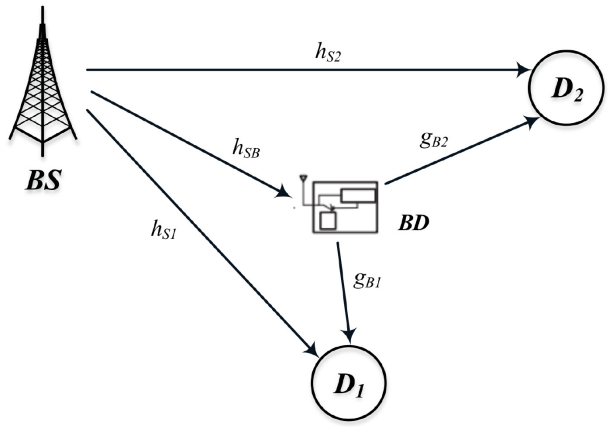

Fig. 1: *System Model.*

We consider in Fig. 1 a downlink backscatter-NOMA system. In this regard, the system contains the base station (BS), BD, and two NOMA users. In term of NOMA users, we divide two kinds such as the nearby cellular user (D_1), and the far-away cellular user (D_2). To conduct NOMA transmission, the BS transmits the superposition signal to D_1 and D_2 at the same resource block with different powers. In the context of AB, the node BD transmits its information to D_1 over the signal received from BS.

In term of NOMA concept, it is noted that D_1 is considered as a IoT reader. In particular, D_1 decodes the information of D_2 first, then its own information, finally detecting the BD's information. This is achieved using successive interference cancellation (SIC) strategy. It is assumed that D_2 decodes its own information only. In what follows, we provide the received signal and signal-to-interference-plus-noise ratio (SINR) models at D_1 and D_2.

2.1 The received signals at D_1

The superposition message at the BS can be written as

$$s = \sqrt{\varepsilon_1 P} s_1 + \sqrt{\varepsilon_2 P} s_2, \tag{1}$$

The BD backscatters the BS's signal to D_1 with its own message $v(t)$, where $\mathrm{E}\left[|v(t)|^2\right] = 1$. Thus, D_1 receives two types of signals: direct link signal from the BS and the backscatter link signal from the BD.

The received signals at D_1 can thus be written as [30], [31]

$$y_{D1} = (h_{S1} + \tau_{S1})\, s + \phi h_{SB} g_{B1} s v(t) + w_1, \tag{2}$$

As mentioned earlier, D_1 first decodes s_2, then s_1, and finally $v(t)$ with SIC technique. When decoding s_2, the SINR is given by

$$\gamma_{S1\leftarrow 2} = \frac{\varepsilon_2 \rho |h_{S1}|^2}{\varepsilon_1 \rho |h_{S1}|^2 + \rho |\phi|^2 |h_{SB}|^2 |g_{B1}|^2 + \rho \kappa_{S1} + 1}, \tag{3}$$

where $\rho = \frac{P}{\varsigma^2}$.

It is assumed that s_2 can be decoded successfully, it can be subtracted from y_{D1}, and then D_1 decodes its own message s_1, in which the SINR is given by

$$\gamma_{S1} = \frac{\varepsilon_1 \rho |h_{S1}|^2}{\rho |\phi|^2 |h_{SB}|^2 |g_{B1}|^2 + \rho \kappa_{S1} + 1}. \tag{4}$$

Further, conditioned on perfectly decoding s_1, the BD message $v(t)$ can then be decoded at D_1 based on SIC technique. Given s, the SNR to decode $v(t)$ at D_1 can be formulated by

$$\gamma_v = \frac{\rho |\phi|^2 |h_{SB}|^2 |g_{B1}|^2}{\rho \kappa_{S1} + 1}. \tag{5}$$

2.2 The received signals at D_2

The received signals at D_2 can be written as

$$y_{D2} = (h_{S2} + \tau_{S2})\, s + \phi h_{SB} g_{B2} s v(t) + w_2, \tag{6}$$

Noted that user D_2 only decodes its own message s_2 by treating other signal components as interference. To decod s_2, the SINR is computed by

$$\gamma_{S2} = \frac{\varepsilon_2 \rho |h_{S2}|^2}{\varepsilon_1 \rho |h_{S2}|^2 + \rho |\phi|^2 |h_{SB}|^2 |g_{B2}|^2 + \rho \kappa_{S2} + 1}. \tag{7}$$

As shown in Fig. 1, if the BS does not serve D_2, the backscatter-NOMA system turns into an AB-NOMA system. In this case, ε_1 is equal to 1, i.e., [30]. The received signal at D_1 in the AB-NOMA system is expressed as (2). In the AB-NOMA system, D_1 first decodes s_1 then $v(t)$ and the corresponding SINR and SNR are given by (4) and (5) with $\varepsilon_1 = 1$, respectively. If the BD does not exist, the backscatter-NOMA system turns into a conventional downlink NOMA system.

In next section, we will analyze the performance for backscatter-NOMA SR system in terms of outage probability. Since the performance of conventional NOMA system has been analyzed in [32], and thus we omit it in this paper.

3. OUTAGE PROBABILITY ANALYSIS

It is necessary to compute expressions of the outage probability to exhibit performance analysis since the target rates of users are determined by their required quality of service (QoS). In particular, we will study the outage probability performance for the AB-NOMA system.

3.1 Outage probability of D_1

To deploy AB-NOMA, if D_1 can not decode s_1 successfully, we define this event as the outage event. The outage probability of D_1 in AB-NOMA is given by [30]

$$\begin{aligned} OP_{D1} &= \Pr\left(\gamma_{S1} < \gamma_{D1}\right) \\ &= 1 - \underbrace{\Pr\left(\gamma_{S1} \geq \gamma_{D1}\right)}_{\Psi}. \end{aligned} \tag{8}$$

Proposition 1. The closed-form expression for the outage probability of D_1 is given by

$$\begin{aligned} OP_{D1} = 1 &+ \frac{\varepsilon_1 \lambda_{S1}}{\gamma_{D1}|\phi|^2 \lambda_{SB} \lambda_{B1}} \\ &\times \exp\left(\frac{\varepsilon_1 \lambda_{S1}}{\gamma_{D1}|\phi|^2 \lambda_{SB} \lambda_{B1}} - \frac{\gamma_{D1}\left(\rho\kappa_{S1}+1\right)}{\varepsilon_1 \rho \lambda_{S1}}\right) \\ &\times \mathrm{Ei}\left(-\frac{\varepsilon_1 \lambda_{S1}}{\gamma_{D1}|\phi|^2 \lambda_{SB} \lambda_{B1}}\right), \end{aligned} \tag{9}$$

where $\gamma_{Di} = 2^{2R_{Di}} - 1$ the target SINR to decode s_i and R_{Di} are the target rate for D_i.

Proof: By definition, Ψ denotes the complementary event at D_1 and is calculated as (10).

Applying [33, Eq. (3.352.4)] and some polynomial expansion manipulations, Ψ can be calculated as

$$\begin{aligned} \Psi = &- \frac{\varepsilon_1 \lambda_{S1}}{\gamma_{D1}|\phi|^2 \lambda_{SB} \lambda_{B1}} \\ &\times \exp\left(\frac{\varepsilon_1 \lambda_{S1}}{\gamma_{D1}|\phi|^2 \lambda_{SB} \lambda_{B1}} - \frac{\gamma_{D1}\left(\rho\kappa_{S1}+1\right)}{\varepsilon_1 \rho \lambda_{S1}}\right) \\ &\times \mathrm{Ei}\left(-\frac{\varepsilon_1 \lambda_{S1}}{\gamma_{D1}|\phi|^2 \lambda_{SB} \lambda_{B1}}\right). \end{aligned} \tag{11}$$

Substituting (11) into (8), (9) can be obtained.

The proof is completed.

3.2 Outage probability of BD

If D_1 fails to decode s_1 or $v(t)$, the outage event for BD occurs, and thus the outage probability of BD can be expressed as [30]

$$\begin{aligned} OP_{BD} &= 1 - \Pr\left(\gamma_{S1} \geq \gamma_{D1}, \gamma_v \geq \gamma_{BD}\right) \\ &= 1 - \underbrace{\Pr\left(\gamma_{S1} \geq \gamma_{D1}\right)}_{\Psi} \underbrace{\Pr\left(\gamma_v \geq \gamma_{BD}\right)}_{A_1}. \end{aligned} \tag{12}$$

where $\gamma_{BD} = 2^{2R_{BD}} - 1$ and R_{BD} is the target rate for BD.

Proposition 2. The closed-form expression for the outage probability of BD without direct link is given by

$$\begin{aligned} OP_{BD} = 1 &+ \frac{\varepsilon_1 \lambda_{S1}}{\gamma_{D1}|\phi|^2 \lambda_{SB} \lambda_{B1}} \\ &\times \exp\left(\frac{\varepsilon_1 \lambda_{S1}}{\gamma_{D1}|\phi|^2 \lambda_{SB} \lambda_{B1}} - \frac{\gamma_{D1}\left(\rho\kappa_{S1}+1\right)}{\varepsilon_1 \rho \lambda_{S1}}\right) \\ &\times \mathrm{Ei}\left(-\frac{\varepsilon_1 \lambda_{S1}}{\gamma_{D1}|\phi|^2 \lambda_{SB} \lambda_{B1}}\right) \\ &\times \sqrt{\frac{4\gamma_{BD}\left(\rho\kappa_{S1}+1\right)}{\rho|\phi|^2 \lambda_{SB} \lambda_{B1}}} K_1\left(\sqrt{\frac{4\gamma_{BD}\left(\rho\kappa_{S1}+1\right)}{\rho|\phi|^2 \lambda_{SB} \lambda_{B1}}}\right). \end{aligned} \tag{13}$$

Proof: By definition, A_1 can be expressed by

$$\begin{aligned} A_1 &= \Pr\left(|h_{SB}|^2 \geq \frac{\gamma_{BD}\left(\rho\kappa_{S1}+1\right)}{\rho|\phi|^2 |g_{B1}|^2}\right) \\ &= \frac{1}{\lambda_{B1}} \int_0^\infty \exp\left(-\frac{\gamma_{BD}\left(\rho\kappa_{S1}+1\right)}{\rho|\phi|^2 \lambda_{SB} x} - \frac{x}{\lambda_{B1}}\right) dx \\ &= \sqrt{\frac{4\gamma_{BD}\left(\rho\kappa_{S1}+1\right)}{\rho|\phi|^2 \lambda_{SB} \lambda_{B1}}} K_1\left(\sqrt{\frac{4\gamma_{BD}\left(\rho\kappa_{S1}+1\right)}{\rho|\phi|^2 \lambda_{SB} \lambda_{B1}}}\right), \end{aligned} \tag{14}$$

where the lase equation follows from the fact that $\int_0^\infty \exp\left(-\frac{\delta}{4x} - \varpi x\right) dx = \sqrt{\frac{\delta}{\varpi}} K_1\left(\sqrt{\delta\varpi}\right)$ in [33, Eq. (3.324)].

By combining (14) and (12), (13) can be obtained and the proof is completed.

3.3 Outage probability of D_2

According to NOMA protocol, we have the outage event if D_2 cannot decode message s_2 successfully. The outage probability of D_2 is expressed as

$$\begin{aligned} OP_{D2} &= \Pr\left(\gamma_{S2} < \gamma_{D2}\right) \\ &= 1 - \underbrace{\Pr\left(\gamma_{S2} \geq \gamma_{D2}\right)}_{\Theta}. \end{aligned} \tag{15}$$

Proposition 3. The closed-form expression for the outage probability of D_2 without direct link is given by

$$\begin{aligned} OP_{D2} = 1 &+ \frac{\left(\varepsilon_2 - \gamma_{D2}\varepsilon_1\right)\lambda_{S2}}{\gamma_{D2}|\phi|^2 \lambda_{SB} \lambda_{B2}} \\ &\times \exp\left(\frac{\left(\varepsilon_2 - \gamma_{D2}\varepsilon_1\right)\lambda_{S2}}{\gamma_{D2}|\phi|^2 \lambda_{SB} \lambda_{B2}} - \frac{\gamma_{D2}\left(\rho\kappa_{S2}+1\right)}{\left(\varepsilon_2 - \gamma_{D2}\varepsilon_1\right)\rho\lambda_{S2}}\right) \\ &\times \mathrm{Ei}\left(-\frac{\left(\varepsilon_2 - \gamma_{D2}\varepsilon_1\right)\lambda_{S2}}{\gamma_{D2}|\phi|^2 \lambda_{SB} \lambda_{B2}}\right). \end{aligned} \tag{16}$$

Proof: By definition, Θ can be formulated by (17).

Using result in [33, Eq. (3.352.4)] and applying

$$\begin{aligned}\Psi &= \Pr\left(|h_{S1}|^2 \geq \frac{\gamma_{D1}\left(\rho|\phi|^2|h_{SB}|^2|g_{B1}|^2+\rho\kappa_{S1}+1\right)}{\varepsilon_1\rho}\right)\\ &= \frac{1}{\lambda_{SB}}\frac{1}{\lambda_{B1}}\exp\left(-\frac{\gamma_{D1}\left(\rho\kappa_{S1}+1\right)}{\varepsilon_1\rho\lambda_{S1}}\right)\int_0^\infty\int_0^\infty \exp\left(-\left(\frac{\gamma_{D1}|\phi|^2 y}{\varepsilon_1\lambda_{S1}}+\frac{1}{\lambda_{SB}}\right)x\right)\exp\left(-\frac{y}{\lambda_{B1}}\right)dxdy \\ &= \frac{1}{\lambda_{B1}}\exp\left(-\frac{\gamma_{D1}\left(\rho\kappa_{S1}+1\right)}{\varepsilon_1\rho\lambda_{S1}}\right)\int_0^\infty \frac{\varepsilon_1\lambda_{S1}}{\gamma_{D1}|\phi|^2\lambda_{SB}y+\varepsilon_1\lambda_{S1}}\exp\left(-\frac{y}{\lambda_{B1}}\right)dy.\end{aligned} \tag{10}$$

$$\begin{aligned}\Theta &= \Pr\left(|h_{S2}|^2 \geq \frac{\gamma_{D2}\left(\rho|\phi|^2|h_{SB}|^2|g_{B2}|^2+\rho\kappa_{S2}+1\right)}{\rho\left(\varepsilon_2-\gamma_{D2}\varepsilon_1\right)}\right)\\ &= \frac{1}{\lambda_{SB}}\frac{1}{\lambda_{B2}}\exp\left(-\frac{\gamma_{D2}\left(\rho\kappa_{S2}+1\right)}{\rho\left(\varepsilon_2-\gamma_{D2}\varepsilon_1\right)\lambda_{S2}}\right)\int_0^\infty\int_0^\infty \exp\left(-\left(\frac{\gamma_{D2}\rho|\phi|^2 y}{\rho\left(\varepsilon_2-\gamma_{D2}\varepsilon_1\right)\lambda_{S2}}+\frac{1}{\lambda_{SB}}\right)x\right)\exp\left(-\frac{y}{\lambda_{B2}}\right)dxdy \\ &= \frac{1}{\lambda_{B2}}\exp\left(-\frac{\gamma_{D2}\left(\rho\kappa_{S2}+1\right)}{\rho\left(\varepsilon_2-\gamma_{D2}\varepsilon_1\right)\lambda_{S2}}\right)\int_0^\infty \frac{\rho\left(\varepsilon_2-\gamma_{D2}\varepsilon_1\right)\lambda_{S2}}{\gamma_{D2}\rho|\phi|^2\lambda_{SB}y+\rho\left(\varepsilon_2-\gamma_{D2}\varepsilon_1\right)\lambda_{S2}}\exp\left(-\frac{y}{\lambda_{B2}}\right)dy.\end{aligned} \tag{17}$$

some further manipulations, Θ can formulated by

$$\begin{aligned}\Theta &= -\frac{\left(\varepsilon_2-\gamma_{D2}\varepsilon_1\right)\lambda_{S2}}{\gamma_{D2}|\phi|^2\lambda_{SB}\lambda_{B2}} \\ &\times \exp\left(\frac{\left(\varepsilon_2-\gamma_{D2}\varepsilon_1\right)\lambda_{S2}}{\gamma_{D2}|\phi|^2\lambda_{SB}\lambda_{B2}}-\frac{\gamma_{D2}\left(\rho\kappa_{S2}+1\right)}{\left(\varepsilon_2-\gamma_{D2}\varepsilon_1\right)\rho\lambda_{S2}}\right) \\ &\times \mathrm{Ei}\left(-\frac{\left(\varepsilon_2-\gamma_{D2}\varepsilon_1\right)\lambda_{S2}}{\gamma_{D2}|\phi|^2\lambda_{SB}\lambda_{B2}}\right).\end{aligned} \tag{18}$$

Combining (18) and (15), (16) can be obtained.

The proof is completed.

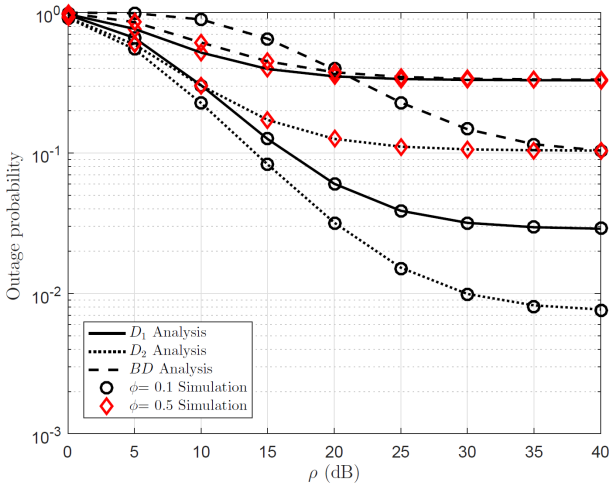

Fig.2: *Outage probabilities versus BS transmit power ρ in AB-NOMA as changing ϕ.*

4. NUMERICAL RESULT

In this section, numerical results are presented to evaluate the proposed performance of the AB-NOMA SR system. Here, the target rates for D_1, D_2, and BD are $R_{D1} = R_{D2} = 0.5$ (bps/Hz), $R_{DB} = 0.1$ (bps/Hz), respectively. In addition, we set $\lambda_{S1} = \lambda_{S2} = \lambda_{SB} = 1$, $\lambda_{B1} = 0.8$, $\lambda_{B1} = 0.2$, $\varepsilon_1 = 0.3$, $\phi = 0.1$, we let $\kappa = \kappa_{S1} = \kappa_{S2} = 0.001$. In this regard, we provide the outage probability performance for the AB-NOMA system.

In Fig. 2, we can see trends of outage probability for three node, D_1, D_2 and BD. Among these cases, D_2 shows its best performance. The main reason is that power allocation factors are different for these nodes. Further, high SNR ρ can improve SINR and then the outage behavior can be improved thoughtfully. Since ϕ leads to higher noise terms to SINR, the corresponding outage performance becomes worse. In this case, $\phi = 0.5$ is reported as worse case.

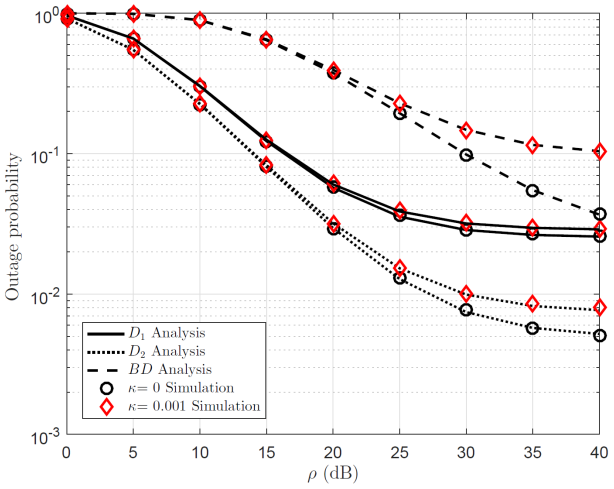

Fig.3: *Outage probabilities versus BS transmit power ρ in AB-NOMA as changing $\kappa = \kappa_{S1} = \kappa_{S2}$.*

We can see the impact of imperfect SIC level to outage performance in Fig. 3. Due to existence of κ coefficient to SINR, then the outage probability depends on such factor κ. In these curves, Monte-Carlo simulation is matched with analytical simulation, which confirms the exactness of derived expressions. Similar trends of three nodes can be observed in this figure.

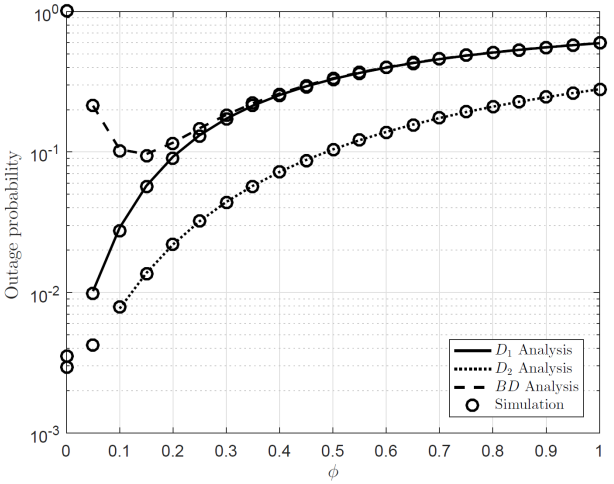

Fig.4: *Outage probabilities versus BS transmit power ϕ in AB-NOMA with $\rho = 40$ (dB).*

We can see the impact of the refection coefficient on outage performance in Fig. 4. Due to existence of ϕ coefficient in the expressions in term of SINR, then the outage probability depends on such factor ϕ. In these curves, significant deduction occurs at these curves due to the impact of he refection coefficient .

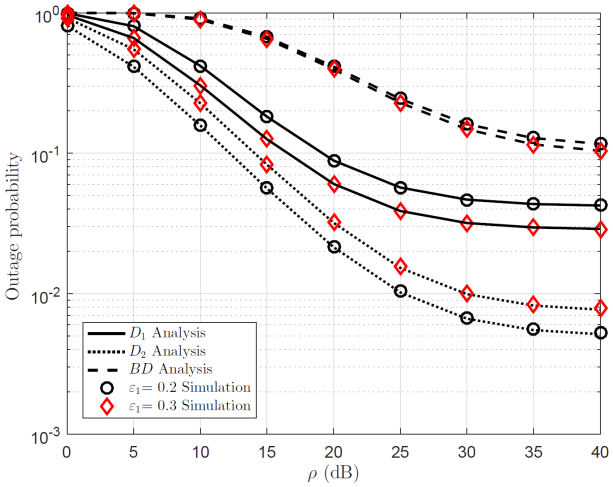

Fig.5: *Outage probabilities versus BS transmit power ρ in AB-NOMA as changing ε_1.*

In Fig. 5, since ε_1 results in different values of SINR for these nodes D_1, D_2 and BD, we can see the impact of the ε_1 on outage performance of user D_1 in Fig. 5. Therefore, we can change SINR to control the outage probability. In these curves, gaps among outage probabilities are resulted by this power factor.

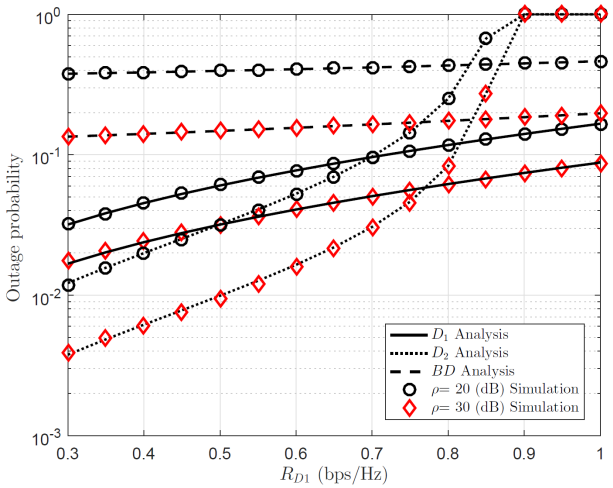

Fig.6: *Outage probabilities versus BS data rate $R_{D1} = R_{D2}$ in AB-NOMA as changing ρ.*

In Fig. 6, since data rate R_{D1} contains in the expressions of SINRs, then outage probability depends on such factor R_{D1}. Therefore, higher value of R_{D1} leads to worse performance. In these curves, the worst performance of outage probability occurs as $R_{D1} = 1$ for user D_2 regardless of transmit SNR ρ.

5. CONCLUSION

This paper has presented performance of three users by exploiting NOMA and AB techniques. It

can be reported that power allocation factors are main factor to outage performance. The transmit SNR at the *BS* contributes to variations of SINR, then the outage probabilities in many situations depend on this factor significantly. As can be seen from results, benefiting from *BD*, the two NOMA users are seen via the gaps since different system parameters assigned for them. The backscatter is important mechanism to improve outage probability for far distant users. The analytical results are matched with Monte-Carlo simulation to show outage probabilities for these main destinations in the AB-NOMA system. Moreover, depending level of imperfect CSI, the outage probability changes to indicate the role of quality of channels in such system.

References

[1] A. Liu, A. N. Parks, V. Talla, , S. Gollakota, D. Wetherall, and J. R, Smith, "Ambient backscatter: wireless communication out of thin air," in *Proc. ACM SIGCOMM*, New York, NY, pp. 39-50, Aug. 2013.

[2] A. N. Parks, A. Liu, S. Gollakota, and J. R, Smith, "Turbocharging ambient backscatter communication," in *Proc. ACM SIGCOMM*, Chicago, USA, pp. 619-630, Aug. 2014.

[3] D. Bharadia, K. R. Joshi, M. Kotaru, and S. Katti, "BackFi: High Throughput WiFi Backscatter," in *Proc. ACM SIGCOMM*, London, pp. 283-296, Aug. 2015.

[4] N. V. Huynh, D. T. Hoang, X. Lu, D. Niyato, P. Wang, and D. I. Kim, "Ambient backscatter communications: A contemporary survey," *IEEE Commun. Surveys Tuts.*, vol. 20, no. 4, pp. 2889-2922, 4th Quart., 2018.

[5] Y. Ye, L. Shi, R. Hu and G. Lu, "Energy-Efficient Resource Allocation for Wirelessly Powered Backscatter Communications," *IEEE Commun. Lett.*, vol. 23, no. 8, pp. 1418-1422, Aug. 2019.

[6] B. Lyu, Z. Yang, H. Guo, F. Tian, and G. Gui, "Relay Cooperation Enhanced Backscatter Communication for Internet-of-Things," *IEEE Internet of Things J.*, vol. 6, no. 2, pp. 2860-2871, Apr. 2019.

[7] D. Darsena, G. Gelli, and F. Verde, "Modeling and Performance Analysis of Wireless Networks With Ambient Backscatter Devices," *IEEE Trans. Wirel. Commun.*, vol. 65, no. 4, pp. 1797-1814, Apr. 2017.

[8] V. Liu, A. Parks, V. Talla, S. Gollakota, D. Wetherall, and J. R. Smith, "Ambient backscatter: Wireless communication out of thin air," in *Proc. ACM SIGCOMM*, Hong Kong, pp. 39-50, Aug. 2013.

[9] R. Long, Y. Liang, H. Guo, G. Yang and R. Zhang, "Symbiotic radio: A new communication paradigm for passive internet of things," *IEEE Internet of Things J.*, vol. 7, no. 2, pp. 1350-1363, Feb. 2020.

[10] X. Kang, Y. Liang and J. Yang, "Riding on the Primary: A New Spectrum Sharing Paradigm for Wireless-Powered IoT Devices," *IEEE Trans. Wireless Commun.*, vol. 17, no. 9, pp. 6335-6347, Sept. 2018.

[11] D. Li, "Backscatter Communication via Harvest-Then-Transmit Relaying," *IEEE Trans. Veh. Technol.*, vol. 69, no. 6, pp. 6843-6847, June 2020.

[12] H. Ding, D. B. da Costa, and J. Ge, "Outage analysis for cooperative ambient backscatter systems," *IEEE Wireless Commun. Lett.*, vol. 9, no. 5, pp. 601-605, May 2020.

[13] Y. Ye, L. Shi, X. Chu and G. Lu, "On the outage performance of ambient backscatter communications," *IEEE Internet of Things J.*, vol. 7, no. 8, pp. 7265-7278, Aug. 2020.

[14] D. Li, H. Zhang and L. Fan, "Adaptive Mode Selection for BackscatterAssisted Communication Systems With Opportunistic SIC," *IEEE Trans. Veh. Technol.*, vol. 69, no. 2, pp. 2327-2331, Feb. 2020.

[15] D. Li, "Hybrid Active and Passive Antenna Selection for BackscatterAssisted MISO Systems," *IEEE Trans. Commun.*, doi: 10.1109/TCOMM.2020.3014917.

[16] D. Li, "Two Birds With One Stone: Exploiting Decode-and-Forward Relaying for Opportunistic Ambient Backscattering," *IEEE Trans. Commun.*, vol. 68, no. 3, pp. 1405-1416, Mar. 2020.

[17] D.-T. Do, M. V. Nguyen, F. Jameel, R. Jäntti and I. S. Ansari, "Performance Evaluation of Relay-Aided CR-NOMA for Beyond 5G Communications," in *IEEE Access*, vol. 8, pp. 134838-134855, 2020.

[18] D-T. Do, T.-L. Nguyen, K. M. Rabie, X. Li and B. M. Lee, "Throughput Analysis of Multipair Two-Way Replaying Networks With NOMA and Imperfect CSI," *IEEE Access*, vol. 8, pp. 128942-128953, 2020.

[19] S. M. R. Islam, N. Avazov, O. A. Dobre, and K. Kwak, "Power-domain non-orthogonal multiple access (NOMA) in 5G systems: Potentials and challenges," *IEEE Commun. Surveys Tuts.*, vol. 19, no. 2, pp. 721–742, 2nd Quart., 2017.

[20] M. Shirvanimoghaddam, M. Dohler, and S. J. Johnson, "Massive nonorthogonal multiple access for cellular IoT: Potentials and limitations," *IEEE Commun. Mag.*, vol. 55, no. 9, pp. 55–61, Sep. 2017.

[21] H.-P. Dang, M.-S. V. Nguyen, Dinh-Thuan Do, H.-L. Pham, B. Selim and G. Kaddoum, "Joint Relay Selection, Full-Duplex and Device-to-Device Transmission in Wireless Powered NOMA Networks," in IEEE Access, vol. 8, pp. 82442-82460, 2020.

[22] M. A. Sedaghat and R. R. Muller, "On user

pairing in uplink NOMA," *IEEE Trans. Wireless Commun.*, vol. 17, no. 5, pp. 3474–3486, May. 2018.

[23] Dinh-Thuan Do and M.-S. Van Nguyen, "Device-to-device transmission modes in NOMA network with and without Wireless Power Transfer," *Computer Communications*, Vol. 139, pp. 67-77, May 2019.

[24] P. D. Diamantoulakis, K. N. Pappi, Z. Ding, and G. K. Karagiannidis, "Wireless-powered communications with non-orthogonal multiple access," *IEEE Trans. Wireless Commun.*, vol. 15, no. 12, pp. 8422–8436, Dec. 2016.

[25] Z. Xiao, L. Zhu, J. Choi, P. Xia, and X.-G. Xia, "Joint power allocation and beamforming for non-orthogonal multiple access (NOMA) in 5G millimeter wave communications," *IEEE Trans. Wireless Commun.*, vol. 17, no. 5, pp. 2961–2974, May. 2018.

[26] J. Guo, X. Zhou, S. Durrani, and H. Yanikomeroglu, "Design of non-orthogonal multiple access enhanced backscatter communication," *IEEE Trans. Wireless Commun.*, vol. 17, no. 10, pp. 6837–6852, Oct. 2018.

[27] G. Yang, X. Xu, and Y.-C. Liang, "Resource allocation in NOMA enhanced backscatter communication networks for wireless powered IoT," *IEEE Wireless Commun. Lett.*, vol. 9, no. 1, pp. 117–120, Jan. 2020.

[28] X. Li, J. Li, and L. Li, "Performance Analysis of Impaired SWIPT NOMA Relaying Networks over Imperfect Weibull Channels," *IEEE Syst. J.*, vol. 14, no. 1, pp. 669–672, 2020.

[29] S. Arzykulov, T. A. Tsiftsis, G. Nauryzbayev and M. Abdallah, "Outage Performance of Cooperative Underlay CR-NOMA With Imperfect CSI," *IEEE Communications Letters*, vol. 23, no. 1, pp. 176-179, Jan. 2019.

[30] Q. Zhang, L. Zhang, Y. Liang and P. Kam, "Backscatter-NOMA: A Symbiotic System of Cellular and Internet-of-Things Networks," *IEEE Access*, vol. 7, pp. 20000-20013, 2019.

[31] F. Kara and H. Kaya, "Improved User Fairness in Decode-Forward Relaying Non-Orthogonal Multiple Access Schemes With Imperfect SIC and CSI," in *IEEE Access*, vol. 8, pp. 97540-97556, 2020.

[32] Z. Ding, Z. Yang, P. Fan, and H. V. Poor, "On the performance of nonorthogonal multiple access in 5G systems with randomly deployed users," *IEEE Signal Process. Lett.*, vol. 21, no. 12, pp. 1501–1505, Dec. 2014.

[33] I. S. Gradshteyn and I. M. Ryzhik, *Table of Integrals, Series, and Products.* 2000.

Minh-Sang Van Nguyen was born in Bentre, Vietnam. He is currently pursuing the master's degree in wireless communications. He has worked with the Industrial University of Ho Chi Minh City, Vietnam. He published over 20 SCI/SCIE journal papers. His research interests include electronic design, signal processing in wireless communications networks, non-orthogonal multiple access, and physical layer security.

Dinh-Thuan Do (Senior Member, IEEE) received the B.S., M. Eng., and Ph.D. degrees from Vietnam National University (VNU-HCMC), in 2003, 2007, and 2013, respectively, all in communications engineering. He was a Visiting Ph.D. Student with the Communications Engineering Institute, National Tsing Hua University, Taiwan, from 2009 to 2010. Prior to joining Ton Duc Thang University, he was a Senior Engineer with VinaPhone Mobile Network, from 2003 to 2009. His research interests include signal processing in wireless communications networks, NOMA, full-duplex transmission, and energy harvesting. Dr. Thuan was a recipient of Golden Globe Award from Vietnam Ministry of Science and Technology in 2015 (Top 10 most excellent scientist nationwide). He is currently serving as an Editor of COMPUTER COMMUNICATIONS (Elservier, an Associate Editor of EURASIP JOURNAL ON WIRELESS COMMUNICATIONS AND NETWORKING (Springer), an Associate Editor of ELECTRONICS and an Editor of KSII TRANSACTIONS ON INTERNET AND INFORMATION SYSTEMS. He was a Lead Guest Editor of the Special Issue "Recent Advances for 5G: Emerging Scheme of NOMA in Cognitive Radio and Satellite Communications" in ELECTRONICS in 2019. He is also serving as Guest Editor of a Special Issue on "Massive sensors data fusion for health-care informatics" in ANNALS OF TELECOMMUNICATIONS (Springer) in 2020, as a Guest Editor of a Special Issue on "Power Domain Based Multiple Access Techniques in Sensor Networks" in INTERNATIONAL JOURNAL OF DISTRIBUTED SENSOR NETWORKS (IJDSN) in 2020 and a Guest Editor of a Special Issue on "UAV-enabled B5G/6G Networks: Emerging Trends and Challenges" in PHYSICAL COMMUNICATION (Elservier), 2020. His publications include over 80 SCIE/SCI-indexed journal articles, over 60 SCOPUS-indexed journal articles and over 50 international conference papers. He is sole author in one textbook and five book chapter.